Infrared magneto-optical properties of (III,Mn)V ferromagetic semiconductors

Jairo Sinova,[1] T. Jungwirth[1,2] J. Kučera,[2] and A. H. MacDonald[1]
[1]*University of Texas at Austin, Physics Department, 1 University Station C1600, Austin Texas 78712-0264, USA*
[2]*Institute of Physics ASCR, Cukrovarnická 10, 162 53 Praha 6, Czech Republic*
(Received 21 January 2003; revised manuscript received 19 March 2003; published 18 June 2003)

We present a theoretical study of the infrared magneto-optical properties of ferromagnetic (III,Mn)V semiconductors. Our analysis combines the kinetic exchange model for (III,Mn)V ferromagnetism with the Kubo linear response theory and the Born approximation estimates for the effect of disorder on the valence-band quasiparticles. We predict a prominent feature in the ac-Hall conductivity at a frequency that varies over the range from 200 to 400 meV, depending on Mn and carrier densities, and is associated with transitions between heavy-hole and light-hole bands. In its zero frequency limit, our Hall conductivity reduces to the $\vec{k}$-space Berry's phase value predicted by a recent theory of the anomalous Hall effect that is able to account quantitatively for experiment. We compute theoretical estimates for magnetic circular dichroism, Faraday rotation, and Kerr effect parameters as a function of Mn concentration and free carrier density. The midinfrared response feature is present in each of these magneto-optical effects.

DOI: 10.1103/PhysRevB.67.235203 PACS number(s): 75.50.Pp, 75.30.Gw

I. INTRODUCTION

Rapid progress has been achieved over the past year in understanding how growth and annealing conditions influence the properties of (III,Mn)V diluted magnetic semiconductor ferromagnets. These advances have led to the realization of samples with higher ferromagnetic transition temperatures and conductivities.[1–3] (III,Mn)V materials have normally been described using a phenomenological model[4–6] in which the valence-band holes of the host (III,V) semiconductor are coupled by exchange and Coulomb interactions to Mn^{2+} local-moment ions with spin $S=5/2$. The properties predicted by this model are most simply understood in the strongly metallic regime for which disorder in the spatial distribution of the Mn^{2+} ions, and other defects of the materials, can be treated perturbatively. These approximations lead to a picture of the materials in which spin-orbit coupling of the valence-band hole subsystem plays a key role[4] in providing detailed explanations for many qualitative effects discovered in experimental studies of thermodynamic and transport phenomena. The model can account quantitatively for the critical temperature,[5,7] strain sensitive magnetic-crystalline anisotropy,[5,8] anisotropic magnetoresistance coefficients,[9] and the strong anomalous Hall effect.[10,11] Golden rule estimates of quasiparticle scattering amplitudes even provide the correct order of magnitude for longitudinal dc conductivities.[9]

In this paper we discuss corresponding theoretical predictions for the infrared magneto-optical properties of these materials. We evaluate magnetic circular dichroism (MCD), Faraday rotation, and Kerr effects in the infrared regime for several different Mn concentrations and carrier densities. From the microscopic point of view, each of these effects reflects the nonzero value of the ac-Hall conductivity, $\sigma_{xy}(\omega)$. Our linear response theory for the Hall conductivity reduces in the zero frequency limit to the $\vec{k}$-space Berry's phase expression that explains dc-Hall effect observations.[10–12]

In metallic ferromagnets, measurements of magneto-optical coefficients on band energy scales provide very detailed information about the influence of broken time-reversal symmetry on itinerant electron quasiparticle states. The appropriate band energy scale for the heavily *p*-doped (III,Mn)V ferromagnets, and for a number of other materials that have been studied recently,[13] is in the infrared. For this reason, we believe that experimental infrared magneto-optical studies of (III,Mn)V ferromagnets are highly desirable; we expect that they will be carried out in the near future and that comparison with the predictions presented here will be very informative in clarifying the physics of these new ferromagnets. They could, for example, reveal deficiencies of the relatively simple theoretical formulation that we employ. The study of the magneto-optical response of these ferromagnets is also potentially interesting for applications, especially if room temperature ferromagnetism is achieved in the future. Magneto-optical properties of the closely related (II,Mn)VI diluted magnetic semiconductor paramagnets[14] have already proved useful from both basic science and application points of view.

Absorption and reflection measurements in the visible range have been used to establish phenomenological estimates for the *p-d* and *s-d* exchange coupling constants in (II,Mn)VI materials, and in establishing the important role of valence-band holes in the (III,Mn)V's.[5,14–17] Photoemission experiments, which explore the deeper electronic structure, have been used to explore the degree of hybridization between the underlying host valence-band and Mn electronic levels, but suffer from being surface sensitive.[18–20] In the infrared regime, recent optical conductivity measurements have uncovered unusual nondrude behavior, including an optical absorption peak[21–24] connected to back-scattering localization effects and to intervalence-band transitions, in agreement with model calculations.[25,26]

We organize the paper as follows. In Sec. II we introduce the Kubo formula description of the ac anomalous Hall con-

ductivity appropriate for the studied (III,Mn)V ferromagnets. In Sec. III we detail the model Hamiltonian and approximations used in our calculations. In Sec. IV we present an analytic evaluation of the anomalous Hall conductivity for the case in which disorder is neglected and the bands are approximated by the four-band spherical model. (The six-band model that we use for numerical calculation reduces to the four-band model in the limit of infinite spin-orbit coupling strength.) The isotropic band dispersion of this model makes analytic calculations possible, although they are still somewhat cumbersome. The details of this calculation, which builds intuition about qualitative properties of the $\sigma_{xy}(\omega)$ curves, are relegated to an appendix. In Sec. V we present the numerical results of the full model Hamiltonian calculation for $\sigma_{xy}(\omega)$ and apply these results to discuss all the common magneto-optical effects available for experiments in the present geometry. We summarize this work and present our conclusions in Sec. VI.

II. THEORETICAL APPROACH

Our theoretical model description starts by coupling the host semiconductor valence-band electrons, described within the $\vec{k}\cdot\vec{p}$ or Kohn-Luttinger (KL) theory, with $S=5/2$ Mn local moments with a semiphenomenological local exchange interaction treated at a mean-field level.[5,8,9,25] At zero temperature this gives rise to valence-bands that are split by an effective exchange field $\vec{h}=N_{Mn^{2+}}SJ_{pd}\hat{z}$, where $N_{Mn^{2+}}$ is the substitutional Mn density and the strength of the exchange coupling is taken to be $J_{pd}=55\ \mathrm{meV\,nm^{-3}}$.[27] We assume in this paper that the magnetization is aligned along the growth $(\hat{z})$ direction by an applied small external magnetic field. We restrict ourselves to the $T=0$ limit, allowing us to neglect scattering off thermal fluctuations in the Mn moments orientation. We assume collinear magnetization in the ground state, ignoring the possibility of disorder induced noncollinearity in the ground state, which is known to be less likely for the strongly metallic (III,Mn)V ferromagnets on which we focus.[28,29]

The linear response theory Kubo formula expression for the real part of the ac-Hall conductivity of disorder-free noninteracting electrons is

$$\mathrm{Re}[\sigma_{xy}(\omega)]=-\frac{e^2\hbar}{m^2}\int\frac{d\vec{k}}{(2\pi)^3}\sum_{n\neq n'}(f_{n',\vec{k}}-f_{n,\vec{k}})\times\frac{\mathrm{Im}[\langle n'\vec{k}|\hat{p}_x|n\vec{k}\rangle\langle n\vec{k}|\hat{p}_y|n'\vec{k}\rangle]}{(\omega-E_{n\vec{k}}+E_{n'\vec{k}})(E_{n\vec{k}}-E_{n'\vec{k}})},\qquad(1)$$

where $|n\vec{k}\rangle$ are the Bloch valence-band states and $E_{n\vec{k}}$ are the Bloch eigenenergies within $\vec{k}\cdot\vec{p}$ theory (we use either six- or four-band models here), m is the bare electron mass, $f_{n,\vec{k}}$ is the Fermi occupation number (0 or 1 at $T=0$) for the state $|n\vec{k}\rangle$, and $\hat{p}/m$ is the $\vec{k}\cdot\vec{p}$ velocity operator obtained[30] by differentiating the $\vec{k}\cdot\vec{p}$ Hamiltonian with respect to the wave vector. In the zero frequency limit, Eq. (1) reduces to the expression used by Jungwirth *et al.*[10,11] to explain the dc-anomalous Hall conductivity of these materials. This recent work suggests that anomalous Hall effects are more quantitatively useful in characterizing itinerant electron ferromagnets than had been previously thought, at least for the present materials. In this paper we extend this advance to finite frequencies.

Even though the Hall conductivity is finite in the absence of disorder, we do anticipate that disorder will influence the $\sigma_{xy}^{\mathrm{AH}}(\omega)$ curves, primarily by broadening out features. The sources of disorder known to be relevant in these materials include positional randomness of the substitutional Mn ions with charge $Q=-e$, random placement of interstitial Mn ions that act as double donors and are believed to be nonparticipants[31] in the ferromagnetic order, and As antisites that also act as having charge $Q=+2e$ and are nonmagnetic. We estimate the influence of disorder on the valence-band quasiparticles by calculating their lifetimes, using Fermi's golden rule including both screened Coulomb and exchange interactions of the valence electrons with the Mn ions and the compensating defects.[9] Including disorder broadening of the quasiparticle spectral functions, the Kubo formula expression for the Hall conductivity becomes

$$\mathrm{Re}[\sigma_{xy}(\omega)]=-\frac{e^2\hbar}{\omega m^2 V}\sum_{\vec{k}n\neq n'}\mathrm{Im}[\langle n'\vec{k}|\hat{p}_x|n\vec{k}\rangle\langle n\vec{k}|\hat{p}_y|n'\vec{k}\rangle]\times\int\frac{d\epsilon}{2\pi}f(\epsilon)A_{n',\vec{k}}(\epsilon)\mathrm{Re}[G^{\mathrm{ret}}_{n,k}(\epsilon+\hbar\omega)]+f(\epsilon)A_{n,\vec{k}}(\epsilon)\mathrm{Re}[G^{\mathrm{adv}}_{n',k}(\epsilon-\hbar\omega)],\qquad(2)$$

where $A_{n,\vec{k}}(\epsilon)=\Gamma_{n\vec{k}}/[(\epsilon-E_{n\vec{k}})^2+\Gamma^2_{n\vec{k}}/4]$ is the disorder-broadened spectral function and G^{ret} and G^{adv} are the advanced and retarded quasiparticle Green's functions with finite lifetime $\Gamma^{-1}_{n\vec{k}}/2$, obtained from the golden rule scattering rates from uncorrelated disorder (see Sec. II). Since we are interested in the first-order effects of disorder in σ_{xy} we approximate the above expression as

$$\mathrm{Re}[\sigma_{xy}(\omega)]=-\frac{e^2\hbar}{m^2 V}\sum_{\vec{k}n\neq n'}(f_{n',\vec{k}}-f_{n,\vec{k}})\frac{\mathrm{Im}[\langle n'\vec{k}|\hat{p}_x|n\vec{k}\rangle\langle n\vec{k}|\hat{p}_y|n'\vec{k}\rangle][\Gamma^2_{n,n'}+\omega(E_{n\vec{k}}-E_{n,\vec{k}'})-(E_{n\vec{k}}-E_{n,\vec{k}'})^2]}{[(\omega-E_{n\vec{k}}+E_{n'\vec{k}})^2+\Gamma^2_{n,n'}][(E_{n\vec{k}}-E_{n'\vec{k}})^2+\Gamma^2_{n,n'}]},\qquad(3)$$

where $\Gamma_{n,n'} \equiv (\Gamma_n + \Gamma_{n'})/2$ and Γ_n are the golden rule scattering rates averaged over band n as in Ref. 25. We use Eq. (3) to evaluate $\sigma_{xy}(\omega)$ below. Note that the dependence of $\sigma_{xy}(\omega)$ on the hole density p and Mn concentration x are implied in Eq. (3) through the dependence on the Fermi energy and the magnitude of the exchange field $|\vec{h}|$. Here $|\vec{h}|$ is determined only by x, i.e., we assume antisite compensation throughout, and E_F is determined from a fixed p and $\vec{h}$. The fact that x and p can be treated as separate variables is a consequence of the compensation of the free carriers induced by the Mn acceptors by defects omnipresent in the low-temperature molecular beam epitaxial thechnique used in the growth of these materials and its control through several annealing procedures.

III. MODEL HAMILTONIAN

In the virtual crystal approximation, the interactions are replaced by their spatial averages, so that the Coulomb interaction vanishes and hole quasiparticles interact with a spatially constant kinetic-exchange field. The unperturbed Hamiltonian for the holes then reads $H_0 = H^L + \vec{h}\cdot\vec{s}$, where H_h is the host band Hamiltonian, and $\vec{s}$ is the envelope-function hole spin operator. The host band part of the Hamiltonian is described via the four- or six-band Kohn-Luttinger model. Choosing the angular momentum quantization direction to be along the z axis, and ordering the $j=3/2$ and $j=1/2$ basis functions according to the list $(-3/2, 1/2, -1/2, -3/2; 1/2, -1/2)$, the Luttinger-Hamiltonian $\hat{H}^L$ has the form[8]

$$\hat{H}^L = \left(\begin{array}{cccc|cc} \mathcal{H}_{hh} & -c & -b & 0 & \frac{b}{\sqrt{2}} & c\sqrt{2} \\ -c^* & \mathcal{H}_{lh} & 0 & b & -\frac{b^*\sqrt{3}}{\sqrt{2}} & -d \\ -b^* & 0 & \mathcal{H}_{lh} & -c & d & -\frac{b\sqrt{3}}{\sqrt{2}} \\ 0 & b^* & -c^* & \mathcal{H}_{hh} & -c^*\sqrt{2} & \frac{b^*}{\sqrt{2}} \\ \hline \frac{b^*}{\sqrt{2}} & -\frac{b\sqrt{3}}{\sqrt{2}} & d^* & -c\sqrt{2} & \mathcal{H}_{so} & 0 \\ c^*\sqrt{2} & -d^* & -\frac{b^*\sqrt{3}}{\sqrt{2}} & \frac{b}{\sqrt{2}} & 0 & \mathcal{H}_{so} \end{array}\right). \tag{4}$$

In the matrix (4) we have highlighted the $j=3/2$ sector. The Kohn-Luttinger eigenenergies are measured down from the top of the valence band, i.e., they are hole energies. For completeness we list the expressions that define the quantities that appear in $\hat{H}^L$:

$$\mathcal{H}_{hh} = \frac{\hbar^2}{2m}[(\gamma_1+\gamma_2)(k_x^2+k_y^2) + (\gamma_1 - 2\gamma_2)k_z^2],$$

$$\mathcal{H}_{lh} = \frac{\hbar^2}{2m}[(\gamma_1-\gamma_2)(k_x^2+k_y^2) + (\gamma_1 + 2\gamma_2)k_z^2],$$

$$\mathcal{H}_{so} = \frac{\hbar^2}{2m}\gamma_1(k_x^2+k_y^2+k_z^2) + \Delta_{so},$$

$$b = \frac{\sqrt{3}\hbar^2}{m}\gamma_3 k_z(k_x - ik_y),$$

$$c = \frac{\sqrt{3}\hbar^2}{2m}[\gamma_2(k_x^2-k_y^2) - 2i\gamma_3 k_x k_y],$$

$$d = -\frac{\sqrt{2}\hbar^2}{2m}\gamma_2[2k_z^2 - (k_x^2+k_y^2)]. \tag{5}$$

We focus here on GaAs for which $\gamma_1 = 6.98$, $\gamma_2 = 2.06$, $\gamma_3 = 2.93$, and $\Delta_{so} = 341$ meV.[32]

We treat the effects of disorder on the hole quasiparticles through a finite lifetime scattering rate $\Gamma_{n\vec{k}}$ calculated by using Fermi's golden rule. For uncorrelated disorder there are two contributions to the transport-weighted scattering rate $\Gamma_{n\vec{k}} = \Gamma_{n\vec{k}}^{\mathrm{Mn}^{2+}} + \Gamma_{n\vec{k}}^{\text{As-anti}}$ due to substitutional Mn impurities and As antisites, given by

$$\Gamma_{n,\vec{k}}^{\mathrm{Mn}^{2+}} = \frac{2\pi}{\hbar} N_{\mathrm{Mn}^{2+}} \sum_{n'} \int \frac{d\vec{k}'}{(2\pi)^3} |M_{n,n'}^{\vec{k},\vec{k}'}|^2 \times \delta(E_{n,\vec{k}} - E_{n',\vec{k}'})(1 - \cos\theta_{\vec{k},\vec{k}'}),$$

and

$$\Gamma_{n,\vec{k}}^{\text{As-anti}}=\frac{2\pi}{\hbar}N_{\text{As-anti}}\sum_{n'}\int\frac{d\vec{k}'}{(2\pi)^3}|\tilde{M}_{n,n'}^{\vec{k},\vec{k}'}|^2 \times\delta(E_{n,\vec{k}}-E_{n'\vec{k}'})(1-\cos\theta_{\vec{k},\vec{k}'}),$$

where the scattering matrix elements are approximated by the expressions (in S.I. units),

$$M_{n,n'}^{\vec{k},\vec{k}'}=J_{pd}S\langle z_{n\vec{k}}|\hat{s}_z|z_{n'\vec{k}'}\rangle -\frac{e^2}{\epsilon_{host}\epsilon_0(|\vec{k}-\vec{k}'|^2+q_{TF}^2)}\langle z_{n\vec{k}}|z_{n'\vec{k}'}\rangle,$$

and

$$\tilde{M}_{n,n'}^{\vec{k},\vec{k}'}=\frac{e^2}{\epsilon_{host}\epsilon_0(|\vec{k}-\vec{k}'|^2+q_{TF}^2)}\langle z_{n\vec{k}}|z_{n'\vec{k}'}\rangle.$$

Here ϵ_{host} is the host semiconductor dielectric constant, $|z_{n\vec{k}}\rangle$ is the six-component envelope-function eigenspinor of the Hamiltonian $\hat{H}^h$, and the Thomas-Fermi screening wave vector $q_{TF}=\sqrt{g(E_F)e^2/(2\epsilon_{host}\epsilon_0)}$, where $g(E_F)$ is the density of states at the Fermi energy, E_F. The interband scattering broadening $\Gamma_{n,n'}$ in Eq. (3) is then calculated by averaging $\Gamma_{n,n'}(\vec{k})\equiv[\Gamma_n(\vec{k})+\Gamma_{n'}(\vec{k})]/2$ over the allowed transitions between bands n and n' as in Ref. 25.

IV. FOUR-BAND SPHERICAL MODEL

In this section we briefly summarize an analytic calculation of $\sigma_{xy}(\omega)$ for a disorder-free four-band model with isotropic bands, the so-called spherical model. This model is realized by taking the spin-orbit coupling to infinity and taking $\gamma_2=\gamma_3$ (equal to 2.5 for GaAs) in the Kohn-Luttinger six-band model of Eq. (4). This yields

$$\hat{H}^{L-4b}=\frac{\hbar^2}{2m_0}\left[\left(\gamma_1+\frac{5}{2}\gamma_2\right)k^2-2\gamma_2(\vec{k}\cdot\vec{j})^2\right], \tag{6}$$

with the antiferromagnetic coupling between the localized moments and the holes given as before by $h\hat{s}_z=(h/3)\hat{j}_z$. From the Hamiltonian in Eq. (6) one can immediately see one of the consequences of a strong spin-orbit coupling: for a Bloch state labeled by wave vector $\vec{k}$, the spin quantization axis at $h=0$ is parallel to $\vec{k}$. It is possible to evaluate $\sigma_{xy}^{4b}(\omega)$ from Eq. (1) in this model to first order in h by completing a straightforward but lengthy exercise in degenerate perturbation theory. This calculation is described in greater detail in Appendix.[33] Here we simply state the final result:

$$\sigma_{xy}^{4b}(\omega)=\int_{-\infty}^{\infty}d\omega'\frac{A_{xy}(\omega')}{\omega-\omega'}, \tag{7}$$

where the spectral function $A_{xy}(\omega)$ is given by different expressions in three different energy intervals. In the intermediate energy range transitions at all wave vectors within the Fermi surface are allowed, whereas in the lower and upper energy intervals only transitions at a fraction of the wave vectors within the Fermi surface contribute to $A_{xy}(\omega)$. Hence, cosidering the upper and lower limits of the heavy-hole and light-hole bands and their respective differences we obtain the three energy intervals that contribute to $A_{xy}(\omega)$ and which determine the fraction of the Fermi volume that contributes to it. For $m_{lh}E_F/\mu-(h/6)m_{lh}/m_{hh}-h/2<\omega<m_{lh}E_F/\mu+(h/6)m_{lh}/m_{hh}+h/2$,

$$A_{xy}(\omega)=-\frac{e^2\sqrt{2\mu\omega/\hbar}}{(2\pi)^2\hbar}\left\{\left[\frac{3}{8}u^2+\frac{h}{4\hbar\omega}\left(\frac{7}{6}u^3-2u\right)\right]\Bigg|_{1-\Delta_+}^{1} +\left[\frac{u}{8}\left(\sqrt{1-\frac{3}{4}u^2}+\frac{3}{2}u\right) -\frac{\sqrt{3}}{12}\arcsin(\sqrt{3}u/2)\right]\Bigg|_{1-\Delta_-}^{1-\Delta_+}+\frac{h}{4\hbar\omega}\left[-u+\frac{7u^3}{12} +\sqrt{1-\frac{3}{4}u^2}\left(\frac{7}{27}+\frac{13u^2}{18}\right)\right]\Bigg|_{1-\Delta_-}^{1-\Delta_+}\right\}, \tag{8}$$

with

$$\Delta_{\pm}=\frac{\frac{h}{2}\left(1+\frac{\xi^2}{3}\right)+\hbar\tilde{\omega}\mp\frac{\xi}{3}\sqrt{h^2\left(1+\frac{\xi^2}{3}\right)-3\hbar^2\tilde{\omega}^2}}{\frac{h}{2}\left(1+\frac{\xi^2}{3}\right)}, \tag{9}$$

$m_{hh}\equiv m_0/(\gamma_1-2\gamma_2)$, $m_{lh}\equiv m_0/(\gamma_1+2\gamma_2)$, $\xi\equiv m_{lh}/m_{lh}$, $\mu\equiv m_{hh}m_{lh}/(m_{hh}+m_{lh})$, and $\tilde{\omega}=\omega-\hbar k_{lh}^2/2\mu$, where k_{lh} is the light-hole band Fermi wave vector in zero exchange field. For $m_{lh}E_F/\mu+(h/6)m_{lh}/m_{hh}+h/2<\omega<m_{hh}E_F/\mu-h/6-(h/2)m_{hh}/m_{lh}$,

$$A_{xy}(\omega)=\frac{e^2}{(2\pi\hbar)}\frac{5}{24\pi}\sqrt{\frac{2\mu\hbar\omega}{\hbar^2}}\frac{h}{\hbar\omega}. \tag{10}$$

For $m_{hh}E_F/\mu-h/6-(h/2)m_{hh}/m_{lh}<\omega<m_{hh}E_F/\mu+h/6+(h/2)m_{hh}/m_{lh}$,

$$A_{xy}(\omega)=-\frac{e^2\sqrt{2\mu\omega/\hbar}}{(2\pi)^2\hbar}\left[\left[\frac{3}{8}u^2+\frac{h}{4\hbar\omega}\left(\frac{7}{6}u^3-2u\right)\right]\Bigg|_{-1}^{1-\tilde{\Delta}_+} +\left[\frac{u}{8}\left(\sqrt{1-\frac{3}{4}u^2}+\frac{3}{2}u\right) -\frac{\sqrt{3}}{12}\arcsin(\sqrt{3}u/2)\right]\Bigg|_{1-\tilde{\Delta}_+}^{1-\tilde{\Delta}_-}+\frac{h}{4\hbar\omega}\left[\frac{7u^3-12u}{12} +\sqrt{\frac{4-4u^2}{4}}\left(\frac{126+351u^2}{486}\right)\right]\Bigg|_{1-\tilde{\Delta}_+}^{1-\tilde{\Delta}_-}\right], \tag{11}$$

with

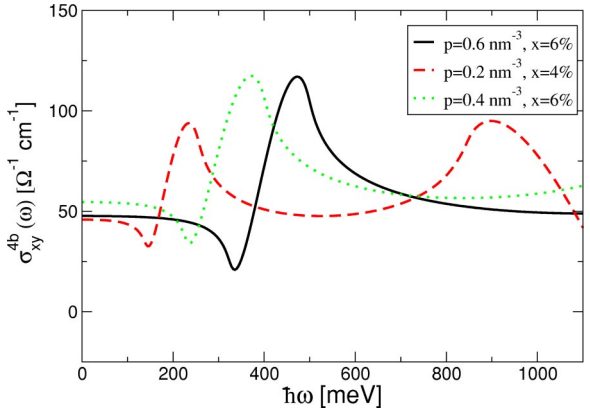

FIG. 1. ac-Hall conductivity calculated within the four-band spherical model without disorder life-time broadening for several itinerant hole and Mn concentrations.

$$\tilde{\Delta}_{\pm}=\frac{\frac{h}{2}\left(1+\frac{\xi^2}{3}\right)+\xi\hbar\tilde{\omega}\mp\frac{\xi}{3}\sqrt{h^2\left(1+\frac{\xi^2}{3}\right)-3\xi^2\hbar^2\tilde{\omega}^2}}{\frac{h}{2}\left(1+\frac{\xi^2}{3}\right)}, \tag{12}$$

and $\tilde{\omega}=\omega-\hbar k_{hh}^2/2\mu$, where k_{hh} is the heavy-hole band Fermi wave vector in zero exchange field; and $A_{xy}(\omega)=0$ otherwise.

We show $\sigma_{xy}^{4b}(\omega)$ for several itinerant hole and Mn concentrations in Fig. 1. From the above result (and from the details presented in the Appendix) it is relatively simple to see the source of the feature observed in the midinfrared regime. The spectral function $A_{xy}(\omega)$, shown in Fig. 2 for the parameters used in Fig. 1, has its major contribution from transitions near the light-holes bands Fermi wave vectors [the lower frequency peak in $A_{xy}(\omega)$] and near the heavy-holes Fermi wave vectors [the higher frequency peak in $A_{xy}(\omega)$], visible for $x=4\%$ and $p=0.2$ nm^{-3}. The transitions that contribute to first order in h are between heavy and light holes with opposite polarization, as shown in the Appendix. We also note that there is a considerable contribution

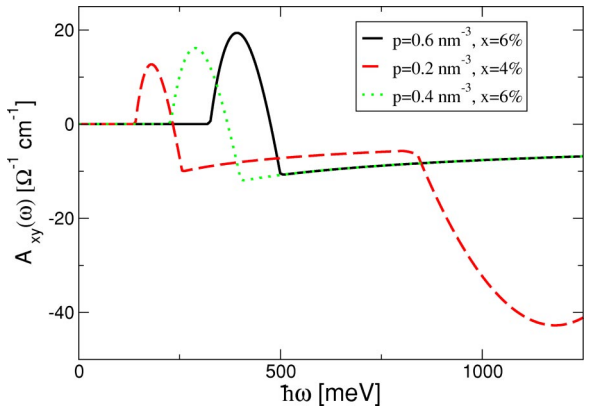

FIG. 2. Spectral function $A_{xy}(\omega)$ calculated within the four-band model the itinerant hole and Mn concentrations of Fig. 1.

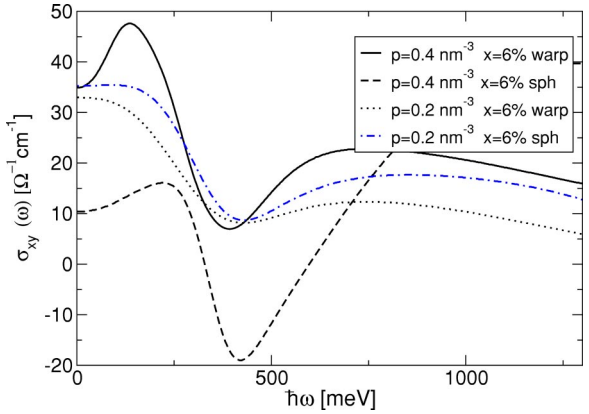

FIG. 3. ac-Hall conductivity $\sigma_{xy}(\omega)$ for $x=6\%$ Mn concentration and $p=0.4$ and 0.2 nm^{-3}, for spherical and nonspherical (band-warping) models.

to $\sigma_{xy}^{4b}(\omega)$ from the high-frequency part of the spectral function (accounts for rigid shifts in the low-frequency range), which indicate the possible need to consider higher bands, maybe including the conduction bands, for more realistic calculations.

V. NUMERICAL RESULTS

The qualitative physics behind the four-band model calculation results still applies to the full model numerical calculations. However, the effects on $\sigma_{xy}(\omega)$ due to the lifetime broadening of the quasiparticles, finite spin-orbit coupling, and the warping of the bands ($\gamma_3\neq\gamma_2$) at higher concentrations are an important part of the quantitative numerical result. Figure 3 shows the anomalous ac-Hall conductivity of disordered system for $x=6\%$ and $p=0.2$ and 0.4 nm^{-3} calculated using the six-band model with warping ($\gamma_3\neq\gamma_2$) and without warping ($\gamma_3=\gamma_2$), which emphasizes the importance of including the warping of the bands in obtaining reliable results that can be compared directly with experiment. Figure 4 shows the ac-Hall conductivity $\sigma_{xy}(\omega)$ for $x=4\%$ Mn concentration and $p=0.2,0.4,0.6$, and 0.8 nm^{-3}. The Hall conductivity must be nonzero in order to have non-

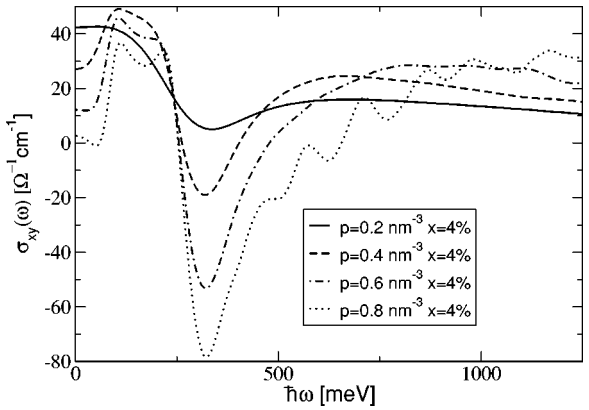

FIG. 4. ac-Hall conductivity $\sigma_{xy}(\omega)$ for $x=4\%$ Mn concentration and $p=0.2,0.4,0.6$, and 0.8 nm^{-3}.

zero magneto-optical effects, but most measurable quantities are also influenced by other elements of the conductivity tensor. The most widely studied magneto-optical effects are the Faraday and Kerr effects. The Faraday effect reflects the relative difference between the optical absorption of right and left circularly polarized light, referred to as MCD. In the Voigt geometry (magnetization aligned with axis of light propagation) and assuming a thin film geometry [applicable for all (III,Mn)V epilayers now available in the infrared regime considered here],[14]

$$\mathrm{MCD}=\frac{\alpha^{+}-\alpha^{-}}{\alpha^{+}+\alpha^{-}}=\frac{\mathrm{Im}[\sigma_{xy}(\omega)]}{\mathrm{Re}[\sigma_{xx}(\omega)]}. \tag{13}$$

Linearly polarized light propagating through a magnetic medium will experience the Faraday rotation of its polarization angle and a transformation from linear to elliptically polarized light due to MCD. The angle of rotation per unit length traversed, again in the thin film geometry, is (in cgs units)[14]

$$\theta_F(\omega)=\frac{4\pi}{(1+n)c}\mathrm{Re}[\sigma_{xy}], \tag{14}$$

where c is the speed of light and n is the index of refraction of the substrate, in this case GaAs with $n=\sqrt{10.9}$. Perhaps the more technologically relevant magneto-optic phenomena is the Kerr effect, which appears in reflection from a magnetic medium. In this case, also within the Voigt geometry, the Kerr angle and ellipticity are defined as[14]

$$\theta_K+i\,\eta_K\equiv\frac{r_{+}-r_{-}}{r_{+}+r_{-}}, \tag{15}$$

where $r_{\pm}$ are the total complex reflection amplitudes (with multiple scattering taken into account) for right and left circular polarized light. Note that the simple relations, $\theta_K \propto \mathrm{Im}[\sigma_{xy}(\omega)]$ and $\eta_K \propto \mathrm{Re}[\sigma_{xy}(\omega)]$,[14] obtained in the thick-layer limit do not apply for the typical thin (III,Mn)V epilayers. In Fig. 5 we show the different magneto-optic effects for a concentration of $x=6\%$ and $p=0.4\ \mathrm{nm}^{-3}$. The Faraday rotation in this case is larger than the giant Faraday rotation observed in the paramagnetic (II,Mn)VI's at optical frequencies[14,34] and should be readily observable in the current highly metallic samples. The Kerr angle and ellipticity we obtain for (Ga,Mn)As are comparable to the Kerr effects observed in the optical regime in materials used for magnetorecording devices.[35] The behavior as a function of free carrier hole concentration can be seen in Fig. 6 where the Faraday rotation angle is shown for several carrier concentrations. The peaks and valleys in the different quantities are present in all the concentrations; however, the magnitude varies, even changing sign at several concentrations and frequencies. Rather than presenting many different graphs for all the possible parameters (p, x, etc.), results for these quantities, together with other physical quantities, can be obtained and plotted vs different nominal parameters.[32]

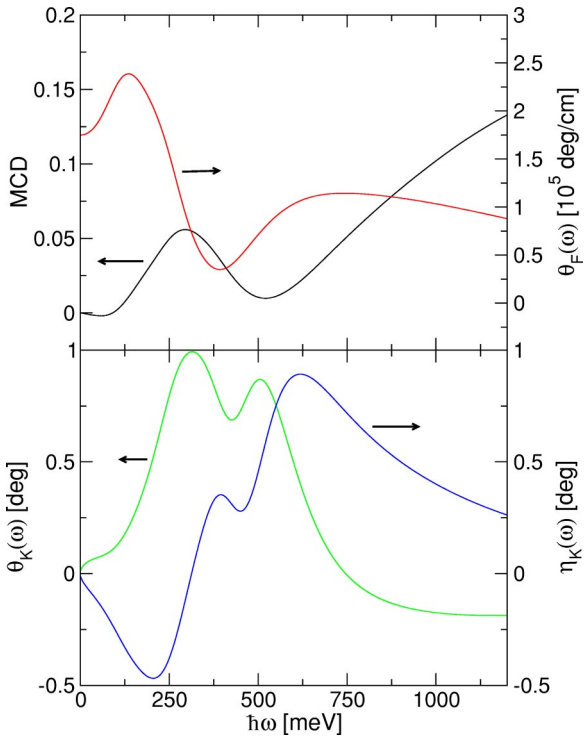

FIG. 5. Faraday and Kerr effects for $x=6\%$ Mn concentration and $p=0.4\ \mathrm{nm}^{-3}$.

VI. CONCLUSIONS

We have presented a theory of the ac-Hall effect in the infrared regime by extending Berry's phase theory of the dc-anomalous Hall effect to finite frequencies and treating the effects of disorder through a finite lifetime of the valence-band quasiparticles. We observe features (peaks and valleys) in the transverse conductivity in the range between 200 and 400 meV at which the conductivity changes by more than 100%. We have studied how these features appear in different magneto-optical effects (MCD, Faraday rotation and Kerr effect) that are relatively easily measured, finding strong signals. The magnitude of the Faraday rotation is very large [one order of magnitude larger than that observed in paramagnetic (II,Mn)VI's, for example] and has a nontrivial dependence on the free carrier concentration. The Kerr effect

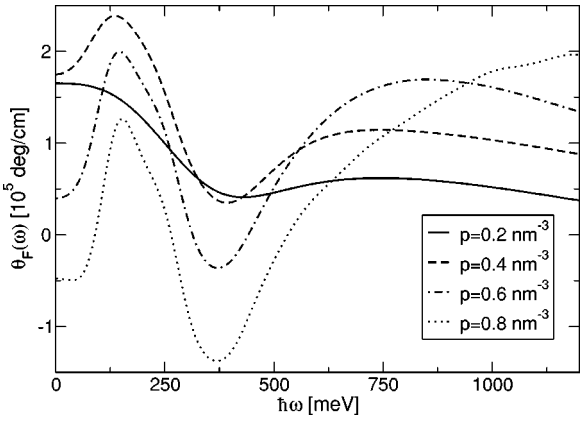

FIG. 6. Faraday rotation angle for $x=6\%$ Mn concentration with $p=0.2,\ 0.4,\ 0.6$, and $0.8\ \mathrm{nm}^{-3}$.

is also strong when compared to materials used in magneto-optic recording. The origin of the peaks is most easily understood within a simple four-band spherical model in which transitions between heavy- and light-hole states with opposite spin polarization give the strongest contribution to the anomalous transverse optical conductivity. The four-band model represents the infinite spin-orbit coupling strength limit of the six-band model we use for numerical calculations. Our use of a six-band model can account only for transitions within the valence-band and not for transitions between conduction and valence-bands. Because of this limitation, we cannot address the crossover between intraband and interband contributions that are not completely separated in these extremely heavily doped semiconductors, something that is clearly desirable and should be addressed in subsequent theoretical work.

Our predictions depend in intricate detail on the model that we have used to describe the ferromagnetism of these materials. The model depends most essentially on the assumption that the Mn impurities act as reasonably shallow acceptors and introduce $S=5/2$ local moment degrees of freedom to the system. The specific calculations presented here assume that Mn impurities and other scatterers in the system can be treated perturbatively. This assumption enables quasiparticle scattering rates to be estimated in a simple way, but is a less essential part of the model. The magneto-optical properties studied here are directly dependent on valence-band spin-orbit coupling, which we have argued elsewhere[4,36] plays an essential role in understanding ferromagnetism in these materials. Confirmation by future experiment of the detailed predictions made here for the magneto-optical properties of these materials would further validate the approach we have taken to modeling these interesting new ferromagnets. We expect that the weak-quasiparticle-scattering approximations made here will be more reliable in more metallic samples, since the scattering rates are then smaller compared to other relevant energy scales, particularly the Fermi energy. We hope that these calculations will help motivate magneto-optic experiments in the infrared regime for (Ga,Mn)As and other (III,Mn)V ferromagnets.

ACKNOWLEDGMENTS

The authors gratefully acknowledge stimulating conversations with D. Basov, B. Gallagher, T. Dietl, and Q. Niu. This work was supported by the Welch Foundation, by the Office of Naval Research under Grant No. N000140010951, and by the Grant Agency of the Czech Republic under Grant No. 202/02/0912.

APPENDIX DERIVATION OF $\sigma_{xy}(\omega)$ IN THE FOUR-BAND SPHERICAL MODEL

We present in this appendix the details involved in deriving the results shown in Eqs. (7)–(12) for the anomalous contribution to the ac-Hall conductivity calculated first in the exchange field within the four-band spherical model. The host valence-band Hamiltonian in this case, as shown in Sec. IV, is given by

$$\hat{H}^{L-4b}=\frac{\hbar^2}{2m_0}\left[\left(\gamma_1+\frac{5}{2}\gamma_2\right)k^2-2\gamma_2(\mathbf{k}\cdot\mathbf{j})^2\right], \tag{A1}$$

The eigenspinors of $\hat{H}^{L-4b}$ are given by

$$|z_{nk}^{(0)}\rangle=e^{-i\hat{j}_z\phi/\hbar}e^{-i\hat{j}_y\theta/\hbar}|n\rangle, \tag{A2}$$

where $|n\rangle$ are the spinors with the axis of quantization along the z-direction and total angular momentum $3/2\hbar$. The perturbation due to the antiferromagnetic coupling to the localized moments is $\hat{H}'=h\hat{s}_z=(h/3)\hat{j}_z$. The eigenvalues to first order in h are then given by

$$E_{hh}^{\pm}=\frac{\hbar^2k^2}{2m_{hh}}\pm\frac{h}{2}\cos\theta \tag{A3}$$

and

$$E_{lh}^{\pm}=\frac{\hbar^2k^2}{2m_{lh}}\pm\frac{h}{3}\sqrt{1-\frac{3}{4}\cos^2\theta}=\frac{\hbar^2k^2}{2m_{lh}}\pm\frac{h}{6}\frac{\cos\theta}{\cos 2\theta'}, \tag{A4}$$

where $\tan 2\theta'=2\tan\theta$, hh labels heavy holes and lh labels light holes. The dipole matrix elements in Eq. (1) are given by

$$\begin{aligned}\langle n'k|\hat{p}_\alpha|nk\rangle&=\frac{m}{\hbar}\left\langle z_{n'k}\left|\frac{\partial H}{\partial k_\alpha}\right|z_{nk}\right\rangle\\&=\frac{m(E_{nk}-E_{n'k})}{\hbar}\left\langle\frac{\partial}{\partial k_\alpha}n'k\middle|nk\right\rangle,\end{aligned} \tag{A5}$$

so we can write

$$\begin{aligned}&\mathrm{Im}[\langle n'k|\hat{p}_x|nk\rangle\langle nk|\hat{p}_y|n'k\rangle]\\&=\frac{m^2}{\hbar^2}(E_{nk}-E_{n'k})^2\mathrm{Im}\left[\left\langle z_{n'k}\left|\frac{\partial}{\partial k_x}z_{nk}\right\rangle\right\langle\frac{\partial}{\partial k_y}z_{nk}\middle|z_{n'k}\right\rangle\right],\end{aligned} \tag{A6}$$

where

$$\begin{aligned}\left|\frac{\partial}{\partial k_x}z_{nk}\right\rangle&=\frac{\cos\phi\cos\theta}{k}\frac{\partial}{\partial\theta}|z_{nk}\rangle-\frac{\sin\phi}{k\sin\theta}\frac{\partial}{\partial\phi}|z_{nk}\rangle\\&+\cos\phi\sin\theta\frac{\partial}{\partial k}|z_{nk}\rangle,\end{aligned} \tag{A7}$$

and similarly

$$\left|\frac{\partial}{\partial k_y} z_{nk}\right\rangle = \frac{\sin\phi\cos\theta}{k}\frac{\partial}{\partial\theta}|z_{nk}\rangle - \frac{\cos\phi}{k\sin\theta}\frac{\partial}{\partial\phi}|z_{nk}\rangle + \sin\phi\sin\theta\frac{\partial}{\partial k}|z_{nk}\rangle. \quad \text{(A8)}$$

The perturbed spinor wave function can be written as

$$\begin{aligned}|z_{nk}\rangle &= \sum_{n'} C^n_{n'}(\theta,k)|z^{(0)}_{n'k}\rangle \\ &= \sum_{n'} C^n_{n'}(\theta,k) e^{-i(\hat{j}_z - j^n(0))\phi/\hbar} e^{-i\hat{j}_y\theta/\hbar}|n'\rangle \\ &\equiv |\tilde{z}_{nk}\rangle - \frac{i}{\hbar}(\cos\phi\hat{j}_y - \sin\phi\hat{j}_x)|n'\rangle, \end{aligned} \quad \text{(A9)}$$

where $j^n(0) \equiv \langle z_{n\mathbf{k}=k\hat{z}}|\hat{j}_z|z_{n\mathbf{k}=k\hat{z}}\rangle$. Inserting Eq. (A9) into Eqs. (A7) and (A8) gives

$$\begin{aligned}\left|\frac{\partial}{\partial k_x} z_{nk}\right\rangle &= \frac{i\sin\phi}{\hbar k\sin\theta}[\hat{j}_z - j^n(0)]|z_{nk}\rangle \\ &\quad - i\frac{\cos\phi\cos\theta}{\hbar k}[(\cos\phi\hat{j}_y - \sin\phi\hat{j}_x)|z_{nk}\rangle + i|z_{\tilde{n}k}\rangle] \\ &\quad + \cos\phi\sin\theta\frac{\partial}{\partial k}|z_{nk}\rangle \end{aligned}$$

$$\begin{aligned}\left|\frac{\partial}{\partial k_y} z_{nk}\right\rangle &= \frac{-i\cos\phi}{\hbar k\sin\theta}[\hat{j}_z - j^n(0)]|z_{nk}\rangle \\ &\quad - i\frac{\sin\phi\cos\theta}{\hbar k}[(\cos\phi\hat{j}_y - \sin\phi\hat{j}_x)|z_{nk}\rangle + i|z_{\tilde{n}k}\rangle] \\ &\quad + \sin\phi\sin\theta\frac{\partial}{\partial k}|z_{nk}\rangle \end{aligned}$$

which can be inserted in Eq. (A6) to yield

$$\begin{aligned}&\mathrm{Im}[\langle n'k|\hat{p}_x|nk\rangle\langle nk|\hat{p}_y|n'k\rangle] \\ &= \frac{m^2}{\hbar^2}(E_{nk} - E_{n'k})^2\langle z_{n'k}|[\hat{j}_z - j^n(0)]|z_{nk}\rangle \\ &\quad \times \mathrm{Im}\left[\frac{\cos\theta}{(\hbar k)^2\sin\theta}\langle z_{n'k}|(\cos\phi\hat{j}_y - \sin\phi\hat{j}_x)|z_{nk}\rangle \right. \\ &\quad \left. + i\hbar\langle z_{n'k}|z_{\tilde{n}k}\rangle + \frac{i}{\hbar k}\left\langle z_{n'k}\left|\frac{\partial z_{nk}}{\partial k}\right\rangle\right], \end{aligned} \quad \text{(A10)}$$

where

$$\begin{aligned}&\langle z_{n'k}|[\hat{j}_z - j^n(0)]|z_{nk}\rangle \\ &= \sum_{n_1 n_2} C^{n'}_{n_1}(\theta,k) C^n_{n_2}(\theta,k)\langle n_1|[\hat{j}_z - j^n(0)]|n_2\rangle, \end{aligned}$$

$$\begin{aligned}&\mathrm{Im}[\langle z_{n'k}|(\cos\phi\hat{j}_y - \sin\phi\hat{j}_x)|z_{nk}\rangle] \\ &= \sum_{n_1 n_2} C^{n'}_{n_1}(\theta,k) C^n_{n_2}(\theta)\langle n_1|\hat{j}_y|n_2\rangle, \end{aligned}$$

$$\langle z_{n'k}|z_{\tilde{n}k}\rangle = \sum_{n_1} C^{n'}_{n_1}(\theta,k)\frac{\partial C^n_{n_1}(\theta,k)}{\partial\theta} \quad \text{and}$$

$$\left\langle z_{n'k}\left|\frac{\partial z_{nk}}{\partial k}\right\rangle = \sum_{n_1} C^{n'}_{n_1}(\theta,k)\frac{\partial C^n_{n_1}(\theta,k)}{\partial k}.\right.$$

Here we only need to consider six transitions since we only need the $n \neq n'$ terms and we will ignore transitions between bands with equal effective masses, which can be shown to contribute to higher order in h. From degenerate perturbation theory we obtain the four eigenvectors to linear order in h:

$$|\mathbf{k}, hh\pm\rangle = |\mathbf{k}, \pm 3/2\rangle + \frac{h\mu\sin\theta}{\sqrt{3}(\hbar k)^2}|\mathbf{k}, \pm 1/2\rangle, \quad \text{(A11)}$$

$$\begin{aligned}|\mathbf{k}, lh+\rangle &= \cos\theta'|\mathbf{k}, +1/2\rangle - \sin\theta'|\mathbf{k}, -1/2\rangle \\ &\quad - \frac{h\mu\sin\theta}{\sqrt{3}(\hbar k)^2}[\cos\theta'|\mathbf{k}, +3/2\rangle - \sin\theta'|\mathbf{k}, -3/2\rangle], \end{aligned} \quad \text{(A12)}$$

$$\begin{aligned}|\mathbf{k}, lh-\rangle &= \sin\theta'|\mathbf{k}, +1/2\rangle + \cos\theta'|\mathbf{k}, -1/2\rangle \\ &\quad - \frac{h\mu\sin\theta}{\sqrt{3}(\hbar k)^2}[\sin\theta'|\mathbf{k}, +3/2\rangle + \cos\theta'|\mathbf{k}, -3/2\rangle], \end{aligned} \quad \text{(A13)}$$

where $\mu \equiv m_{lh}m_{hh}/(m_{hh} - m_{lh})$. The Fermi wave vectors to first order in h/E_F for each band are given by

$$k_F^{hh\pm}(\theta) = k_F^{hh(0)}\left(1 \pm \frac{h}{4E_F}\cos\theta\right) \quad \text{and}$$

$$k_F^{lh\pm}(\theta) = k_F^{lh(0)}\left(1 \pm \frac{h}{6E_F}\sqrt{1 - \frac{3}{4}\cos^2\theta}\right). \quad \text{(A14)}$$

After some lengthy algebra one obtains

$$\frac{\mathrm{Im}[\langle k,hh+|\hat{p}_x|k,lh+\rangle\langle k,lh+|\hat{p}_y|k,hh+\rangle]}{(E^+_{lh}-E^+_{hh})} = \frac{3m^2}{8\mu}\cos\theta\cos^2\theta' + \frac{hm^2}{2(\hbar k)^2}\left[-\frac{1}{4}\sin(2\theta)\sin(2\theta') + \cos 2\theta\cos^2\theta' + \frac{\cos^2\theta\cos^2\theta'}{4\cos 2\theta'} - \frac{3}{4}\cos^2\theta\cos^2\theta'\right], \tag{A15}$$

$$\frac{\mathrm{Im}[\langle k,hh+|\hat{p}_x|k,lh-\rangle\langle k,lh-|\hat{p}_y|k,hh+\rangle]}{(E^-_{hl}-E^+_{hh})} = \frac{3m^2}{8\mu}\cos\theta\sin^2\theta' + \frac{hm^2}{2(\hbar k)^2}\left[+\frac{1}{4}\sin(2\theta)\sin(2\theta') + \cos 2\theta\sin^2\theta' - \frac{\cos^2\theta\sin^2\theta'}{4\cos 2\theta'} - \frac{3}{4}\cos^2\theta\sin^2\theta'\right], \tag{A16}$$

$$\frac{\mathrm{Im}[\langle k,hh-|\hat{p}_x|k,lh+\rangle\langle k,lh+|\hat{p}_y|k,hh-\rangle]}{(E^+_{hl}-E^-_{hh})} = -\frac{3m^2}{8\mu}\cos\theta\sin^2\theta' + \frac{hm^2}{2(\hbar k)^2}\left[+\frac{1}{4}\sin(2\theta)\sin(2\theta') + \cos 2\theta\sin^2\theta' - \frac{\cos^2\theta\sin^2\theta'}{4\cos 2\theta'} - \frac{3}{4}\cos^2\theta\sin^2\theta'\right], \tag{A17}$$

$$\frac{\mathrm{Im}[\langle k,hh-|\hat{p}_x|k,lh-\rangle\langle k,lh-|\hat{p}_y|k,hh-\rangle]}{(E^-_{lh}-E^-_{hh})} = -\frac{3m^2}{8\mu}\cos\theta\cos^2\theta' + \frac{hm^2}{2(\hbar k)^2}\left[-\frac{1}{4}\sin(2\theta)\sin(2\theta') + \cos 2\theta\cos^2\theta' + \frac{\cos^2\theta\cos^2\theta'}{4\cos 2\theta'} - \frac{3}{4}\cos^2\theta\cos^2\theta'\right]. \tag{A18}$$

Using Eqs. (A15)–(A18) we can compute directly the dc conductivity [Eq. (1) for $\omega=0$]:

$$\sigma_{xy}(0) = \frac{2e^2\hbar}{m^2V}\sum_{\mathbf{k},n>n'} \times\frac{(f_{n',k}-f_{n,k})\mathrm{Im}[\langle n'k|\hat{p}_x|nk\rangle\langle nk|\hat{p}_y|n'k\rangle]}{(E_{nk}-E_{n'k})^2} = -\frac{e^2}{(2\pi\hbar)}\frac{hk^{hh0}_F}{4\pi E_F}\left[1-\frac{1}{3}\sqrt{\frac{m_{lh}}{m_{hh}}} + \frac{8}{3}\frac{m_{lh}}{m_{lh}+\sqrt{m_{lh}m_{hh}}}\right], \tag{A19}$$

in agreement with the previously derived dc-anomalous Hall conductivity,[10] using Berry's phase contribution to the Bloch group velocity in the semiclassical equations of motion approach.

To compute the ac-anomalous Hall conductivity given by Eq. (1), we rewrite it in terms of the spectral function $A_{xy}(\omega)$:

$$\sigma_{xy}(\omega) = \int_{-\infty}^{\infty} d\omega' \frac{A_{xy}(\omega')}{\omega-\omega'}, \tag{A20}$$

with

$$A_{xy}(\omega) \equiv -\frac{e^2\hbar}{m^2V}\sum_{\mathbf{k},n\neq n'}\frac{(f_{n',k}-f_{n,k})\mathrm{Im}[\langle n'k|\hat{p}_x|nk\rangle\langle nk|\hat{p}_y|n'k\rangle]}{(E_{nk}-E_{n'k})}\delta[\hbar\omega-(E_{nk}-E_{n'k})]. \tag{A21}$$

$A_{xy}(\omega)$ is an odd function of ω and we need only to consider $\omega>0$. We need to consider three separate frequency ranges in what follows. First we look at the range

$$\frac{m_{lh}E_F}{\mu}+\frac{m_{lh}}{m_{hh}}\frac{h}{6}+\frac{h}{2}<\omega<\frac{m_{hh}E_F}{\mu}-\frac{h}{6}-\frac{m_{hh}}{m_{lh}}\frac{h}{2}, \tag{A22}$$

and consider the different contributions to $A_{xy}(\omega)$ from the four types of transitions, $hh^{\pm}\rightarrow lh^{\pm}$, separately. For $hh+$ to $lh\pm$ transitions, we have

$$A_{xy}(\omega;hh+\rightarrow lh\pm)$$
$$=-\frac{e^2\hbar}{m^2(2\pi)^2}\int_{-1}^{1}d(\cos\theta)\frac{\mu k\,\mathrm{Im}[\langle k,hh+|\hat{p}_x|k,lh\pm\rangle\langle k,lh\pm|\hat{p}_y|k,hh+\rangle]}{\hbar^2(E_{hl}^{\pm}-E_{hh}^{+})}\Bigg|_{k=\sqrt{\frac{2\mu\omega}{\hbar}}(1\mp\frac{h\cos\theta}{12\hbar\omega\cos 2\theta'}+\frac{h}{4\hbar\omega}\cos\theta)}$$
$$=-\frac{e^2\sqrt{2\mu\omega/\hbar}}{(2\pi)^2\hbar}\int_{-1}^{1}d(\cos\theta)\left(\frac{3}{8}\cos\theta\begin{Bmatrix}\cos^2\theta'\\ \sin^2\theta'\end{Bmatrix}+\frac{h}{4\hbar\omega}\left[\mp\frac{1}{4}\sin(2\theta)\sin(2\theta')+\cos 2\theta\begin{Bmatrix}\cos^2\theta'\\ \sin^2\theta'\end{Bmatrix}\right.\right.$$
$$\left.\left.\times\pm\frac{1}{8}\frac{\cos^2\theta}{\cos 2\theta'}\begin{Bmatrix}\cos^2\theta'\\ \sin^2\theta'\end{Bmatrix}-\frac{3}{8}\cos^2\theta\begin{Bmatrix}\cos^2\theta'\\ \sin^2\theta'\end{Bmatrix}\right]\right).$$

We can sum the two and obtain

$$A_{xy}(\omega;hh+\rightarrow lh+)+A_{xy}(\omega;hh+\rightarrow lh-)$$
$$=-\frac{e^2\sqrt{2\mu\omega/\hbar}}{(2\pi)^2\hbar}\int_{-1}^{1}d(\cos\theta)\left[\frac{3}{8}\cos\theta+\frac{h}{4\hbar\omega}\left(+\cos 2\theta+\frac{1}{8}\cos^2\theta-\frac{3}{8}\cos^2\theta\right)\right]$$
$$=\frac{e^2}{(2\pi\hbar)}\frac{5}{48\pi}\sqrt{\frac{2\mu\hbar\omega}{\hbar^2}}\frac{h}{\hbar\omega}. \quad \text{(A23)}$$

For the $hh-$ to $lh\pm$ transition we obtain the same result, therefore within this range we have

$$A_{xy}(\omega)=\frac{e^2}{(2\pi\hbar)}\frac{5}{24\pi}\sqrt{\frac{2\mu\hbar\omega}{\hbar^2}}\frac{h}{\hbar\omega}.$$

As one can see from its definition $A_{xy}(\omega)$ changes most rapidly in the region where transitions near the Fermi surface are allowed. Let us next consider transitions from $hh+$ to $lh\pm$ first in the lower range $(m_{lh}/\mu)E_F-(m_{lh}/m_{hh})(h/6)-h/2<\omega<(m_{lh}/\mu)E_F+(m_{lh}/m_{hh})(h/6)+h/2$:

$$A_{xy}(\omega;hh+\rightarrow lh\pm)=\int_{-1}^{1}d(\cos\theta)\int_{k_F^{lh\pm}(\theta)}^{\infty}dk f(\theta,k)\,\delta(\hbar\omega-\Delta E^{\pm}), \quad \text{(A24)}$$

with

$$\Delta E_{+}^{\pm}=\frac{(\hbar k)^2}{2\mu}\pm\frac{h\cos\theta}{6\cos 2\theta'}-\frac{h}{2}\cos\theta \quad \text{and}$$

$$k_F^{lh\pm}(\theta)=k_F^{lh(0)}\left(1\mp\frac{h}{6E_F}\sqrt{1-\frac{3}{4}\cos^2\theta}\right).$$

The minimum of $\Delta E^{\pm}(\theta)_{+}$ at a fixed θ is then

$$\Delta E_{+}^{\pm}(\theta)=\frac{\hbar^2}{2\mu}k_F^{lh(0)2}\pm\xi\frac{h\cos\theta}{6\cos 2\theta'}-\frac{h}{2}\cos\theta, \quad \text{(A25)}$$

where we have defined $\xi=-m_{lh}/\mu+1=m_{lh}/m_{hh}$, and the absolute minimum is given by

$$\Delta E_{+}^{\pm}(\theta_{min}=0)=\frac{\hbar^2}{2\mu}k_F^{lh(0)2}\pm\frac{m_{lh}}{m_{hh}}\frac{h}{6}-\frac{h}{2}.$$

For $hh-$ to $lh\pm$ we have instead

$$\Delta E_{-}^{\pm}(\theta)=\frac{\hbar^2}{2\mu}k_F^{lh(0)2}\pm\frac{m_{lh}}{m_{hh}}\frac{h\cos\theta}{6\cos 2\theta'}+\frac{h}{2}\cos\theta,$$

$$\Delta E_{-}^{\pm}(\theta_{min}=\pi)=\frac{\hbar^2}{2\mu}k_F^{lh(0)2}\pm\frac{m_{lh}}{m_{hh}}\frac{h}{6}-\frac{h}{2}.$$

Let $\hbar\omega=(\hbar^2/2\mu)k_F^{lh(0)2}+\tilde{\omega}$, where $\hbar\tilde{\omega}$ will be of the order of h. For an $\tilde{\omega}$, which is too small, there will be a limit on the angular integration $\tilde{\theta}$ obtained by setting $k=k_F^{lh\pm}$, so for $hh+$ to $lh\pm$,

$$\hbar\tilde{\omega}\mp\frac{m_{lh}}{m_{hh}}\frac{h}{3}\sqrt{1-\frac{3}{4}\cos^2\tilde{\theta}}+\frac{h}{2}\cos\tilde{\theta}=0, \quad \text{(A26)}$$

whose solution is

$$\cos\tilde{\theta}_{\pm}=\frac{-\hbar\tilde{\omega}\pm\frac{\xi}{3}\sqrt{h^2\left(1+\frac{\xi^2}{3}\right)-3\hbar^2\tilde{\omega}^2}}{\frac{h}{2}\left(1+\frac{\xi}{3}\right)}\equiv 1-\Delta_{\pm}, \quad \text{(A27)}$$

A similar procedure for the transitions from $hh-$ to $lh\pm$ yields $\cos\tilde{\theta}_{\pm}=-1+\Delta_{\mp}$. Combining the contributions for each transition we then obtain, for $m_{lh}E_F/\mu-(h/6)m_{lh}/m_{hh}-h/2<\omega<m_{lh}E_F/\mu+(h/6)m_{lh}/m_{hh}+h/2$,

$$
\begin{aligned}
A_{xy}(\omega) &= \int_{1-\Delta_+}^{1} d(\cos\theta) A_{xy}(\omega,\cos\theta;hh+\rightarrow lh+) + \int_{1-\Delta_-}^{1} d(\cos\theta) A_{xy}(\omega,\cos\theta;hh+\rightarrow lh-) \\
&\quad + \int_{-1}^{-1+\Delta_-} d(\cos\theta) A_{xy}(\omega,\cos\theta;hh-\rightarrow lh+) + \int_{-1}^{-1+\Delta_+} d(\cos\theta) A_{xy}(\omega,\cos\theta;hh-\rightarrow lh-) \\
&= -\frac{e^2\sqrt{2\mu\omega/\hbar}}{(2\pi)^2\hbar}\int_{1-\Delta_+}^{1} d(\cos\theta)\left(\frac{3}{4}\cos\theta\cos^2\theta' + \frac{h}{4\hbar\omega}\left[-\frac{1}{2}\sin(2\theta)\sin(2\theta') + 2\cos 2\theta\cos^2\theta'\right.\right. \\
&\quad \left.\left. + \frac{\cos^2\theta\cos^2\theta'}{4\cos 2\theta'} - \frac{3}{4}\cos^2\theta\cos^2\theta'\right]\right) - \frac{e^2\sqrt{2\mu\omega/\hbar}}{(2\pi)^2\hbar}\int_{1-\Delta_-}^{1} d(\cos\theta)\left(\frac{3}{4}\cos\theta\sin^2\theta'\right. \\
&\quad \left. + \frac{h}{4\hbar\omega}\left[+\frac{1}{2}\sin(2\theta)\sin(2\theta') + 2\cos 2\theta\sin^2\theta' - \frac{\cos^2\theta\sin^2\theta'}{4\cos 2\theta'} - \frac{3}{4}\cos^2\theta\sin^2\theta'\right]\right) \\
&= -\frac{e^2\sqrt{2\mu\omega/\hbar}}{(2\pi)^2\hbar}\left\{\left[\frac{3}{8}u^2 + \frac{h}{4\hbar\omega}\left(\frac{7}{6}u^3 - 2u\right)\right]\right|_{1-\Delta_+}^{1} + \left[\frac{u}{8}\left(\sqrt{1-\frac{3}{4}u^2} + \frac{3}{2}u\right) - \frac{\sqrt{3}}{12}\arcsin(\sqrt{3}u/2)\right]\Bigg|_{1-\Delta_-}^{1-\Delta_+} \\
&\quad + \frac{h}{4\hbar\omega}\left|\left[-u + \frac{7u^3}{12} + \sqrt{1-\frac{3}{4}u^2}\left(\frac{7}{27} + \frac{13u^2}{18}\right)\right]\right|_{1-\Delta_-}^{1-\Delta_+}\Bigg\}.
\end{aligned}
$$

A similar procedure for the upper range $m_{hh}E_F/mu - h/6 - (h/2)m_{hh}/m_{lh} < \omega < m_{hh}E_F/mu + h/6 + (h/2)m_{hh}/m_{lh}$ yields $A_{xy}(\omega)$ given in Eq. (11). For any other value of ω, $A_{xy}(\omega) = 0$.

[1] K. Edmonds, K. Wang, R. Campion, A. Neumann, N. Farley, B. Gallagher, and C. Foxon, Appl. Phys. Lett. **81**, 4991 (2002).

[2] K.C. Ku, S.J. Potashnik, R.F. Wang, M.J. Seong, E. Johnston-Halperin, R.C. Meyers, S.H. Chun, A. Mascarenhas, A.C. Gossard, D.D. Awschalom, P. Schifer and N. Samarth, Appl. Phys. Lett. **82**, 2302 (2003).

[3] I. Kuryliszyn, T. Wojtowicz, X. Liu, J. Furdyna, W. Dobrowolski, J.-M. Broto, M. Goiran, O. Portugall, H. Rakoto, and B. Raquet, cond-mat/0207354 (unpublished).

[4] J. Konig, J. Schliemann, T. Jungwirth, and A. H. MacDonald, in *Electronic Structure and Magnetism of Complex Materials*, edited by D. Singh and D. Papaconstantopoulos (Springer Verlag, Berlin, 2002); http://arXiv. org/abs/cond-mat/0111314 (unpublished).

[5] T. Dietl, H. Ohno, and F. Matsukura, Phys. Rev. B **63**, 195205 (2001).

[6] T. Dietl, H. Ohno, F. Matsukura, J. Cibert, and D. Ferrand, Science (Washington, DC, U.S.) **287**, 1019 (2000).

[7] T. Jungwirth, J. Konig, J. Sinova, J. Kucera, and A. MacDonald, Phys. Rev. B **66**, 012402 (2002).

[8] M. Abolfath, T. Jungwirth, J. Brum, and A.H. MacDonald, Phys. Rev. B **63**, 054418 (2001).

[9] T. Jungwirth, M. Abolfath, J. Sinova, J. Kučera, and A.H. MacDonald, Appl. Phys. Lett. **81**, 4029 (2002).

[10] T. Jungwirth, G. Niu, and A. MacDonald, Phys. Rev. Lett. **88**, 207208 (2002).

[11] T. Jungwirth, J. Sinova, K. Y. Wang, K. W. Edmonds, R. P. Campion, B. L. Gallagher, C. T. Foxon, Q. Niu, and A. H. MacDonald, Appl. Phys. Lett (to be published).

[12] G. Sundaram and Q. Niu, Phys. Rev. B **59**, 14 915 (1999).

[13] See for example, S. Broderick, L. Degiorgi, H. R. Ott, J. L. Sarrao, and Z. Fisk, Eur. Phys. J. B **27**, 3 (2002); Yu.P. Sukhorukov, E. A. Gan'shina, B. I. Belevtsev, N. N. Loshkareva, A. N. Vinogradov, K. D. D. Rathnayaka, A. Parasiris, and D. G. Naugle, J. Appl. Phys. **91**, 4402 (2002); S. Kimura, F. Arai, and M. Ikezawa, J. Phys. Soc. Jpn. **69**, 647 (2000).

[14] K. Ando, in *Magneto-Optics*, edited by S. Sugano and N. Kojima (Springer-Verlag, Berlin, 2000).

[15] K. Ando, T. Hayashi, M. Tanaka, and A. Twardowski, J. Appl. Phys. **83**, 6548 (1998).

[16] J. Szczytko, W. Mac, A. Twardowski, F. Matsukura, and H. Ohno, Phys. Rev. B **59**, 12 935 (1999).

[17] B. Beshchoten, P. Crowell, I. Malajovich, and D. Awschalom, Phys. Rev. Lett. **83**, 3073 (1999).

[18] J. Okobayashi, A. Kimura, T. Mizokawa, A. Fujimori, T. Hayashi, and M. Tanaka, Phys. Rev. B **59**, R2486 (1999).

[19] J. Okobayashi, T. Mizokawa, D. Sarma, A. Fujimori, T. Slupinski, A. Oiwa, and H. Munekata, Phys. Rev. B **65**, 161203 (2002).

[20] J. Okobayashi, A. Kimura, O. Rader, T. Mizokawa, A. Fujimori, T. Hayashi, and M. Tanaka, Phys. Rev. B **64**, 125304 (2001).

[21] E. Singley, R. Kawakami, D. Awschalom, and D. Basov, Phys. Rev. Lett. **89**, 097203 (2002).

[22] K. Hirakawa, S. Katsumoto, T. Hayashi, Y. Hashimoto, and Y. Iye, Phys. Rev. B **65**, 193312 (2002).

[23] S. Katsumoto, T. Hayashi, Y. Hashimoto, Y. Iye, Y. Ishiwata, M. Watanabe, R. Eguchi, T. Takeuchi, Y. Harada, S. Shin, *et al.*, Mater. Sci. Eng., B **84**, 88 (2001).

[24] Y. Nagai, T. Kunimoto, K. Nagasaka, H. Nojiri, M. Motokawa, F.

Matsukura, T. Dietl, and H. Ohno, Jpn. J. Appl. Phys., Part 1 **40**, 6231 (2001).
[25] J. Sinova, T. Jungwirth, S.-R.E. Yang, J. Kucera, and A.H. MacDonald, Phys. Rev. B **66**, 041202 (2002).
[26] S.-R.E. Yang and A.H. MacDonald, Phys. Rev. B **67**, 155202 (2003).
[27] H. Ohno, J. Magn. Magn. Mater. **200**, 110 (1999).
[28] J. Schliemann and A.H. MacDonald, Phys. Rev. Lett. **88**, 137201 (2002).
[29] G. Zarand and B. Janko, Phys. Rev. Lett. **82**, 047201 (2002).
[30] S.-R.E. Yang, J. Sinova, Y. Shim, and A.H. MacDonald, Phys. Rev. B **67**, 045205 (2003).
[31] J. Blinowski and P. Kacman, cond-mat/0212093 (unpublished).
[32] A large database that details our predictions for other host semiconductors over a wide range of compositions and strains, together with predictions for other physical quantities, is available on the internet at http://unix12. fzu. cz/ms/index. php; in the event that the database is temporarely not accessable please contact J. Sinova or T. Jungwirth.
[33] Energetic readers will discover that these calculations start with very long expressions but reach a relatively concise conclusion.
[34] T. Koyanagi, K. Matsubara, H. Takaoka, and T. Takagi, J. Appl. Phys. **61**, 3020 (1987).
[35] M. Kaneko, in *Magneto-Optics*, edited by S. Sugano and N. Kojima (Springer-Verlag, Berlin, 2000).
[36] J. Konig, T. Jungwirth, and A.H. MacDonald, Phys. Rev. B **64**, 184423 (2001).